# Trafficking and Intracellular ATPase Activity of Human Ecto-nucleotidase NTPDase3 and the Effect of ER-Targeted NTPDase3 on Protein Folding[†]

Vasily V. Ivanenkov,[‡] Jean Sévigny,[§] and Terence L. Kirley*[,‡]

*Department of Pharmacology and Cell Biophysics, College of Medicine, University of Cincinnati, P.O. Box 670575, Cincinnati, Ohio 45267-0575, and Centre de Recherche en Rhumatologie et Immunologie, Centre Hospitalier Universitaire de Québec, Université Laval, Québec, QC, Canada*

*Received March 7, 2008; Revised Manuscript Received June 26, 2008*

ABSTRACT: Ecto-nucleoside triphosphate diphosphohydrolases, NTPDase1 (CD39) and NTPDase3, are integral plasma membrane proteins that hydrolyze extracellular nucleotides, thereby modulating the function of purinergic receptors. During processing in the secretory pathway, the active sites of ecto-nucleotidases are located in the lumen of vesicular compartments, thus raising the question whether the ecto-nucleotidases affect the ATP-dependent processes in these compartments, including protein folding in the endoplasmic reticulum (ER). It has been reported (*J. Biol. Chem.* (2001) *276*, 41518−41525) that CD39 is not active until it reaches the plasma membrane, suggesting that terminal glycosylation in Golgi is critical for its activity. To investigate the subcellular location and the mechanism of ecto-nucleotidase activation, we expressed human NTPDase3 in COS-1 cells and blocked the secretory transport with monensin or brefeldin A, or by targeting to ER with a signal peptide. Cell surface biotinylation, sensitivity to glycosidases, and fluorescence microscopy analyses suggest that, in contrast to the previous report on CD39, NTPDase3 becomes catalytically active in the ER or in the ER-Golgi intermediate compartment, and that terminal glycosylation in Golgi is not essential for activity. Moreover, ER-targeted NTPDase3, but not wild-type NTPDase3 or ER-targeted inactive G221A mutant, significantly diminished the folding efficiency and the transport to the plasma membrane of coexpressed CD39 used as a reporter protein. These data suggest that ER-targeted NTPDase3 significantly depletes ATP in ER, whereas wild-type NTPDase3 is likely to acquire ATPase activity in a post-ER, but pre-Golgi, compartment, thus avoiding unproductive ATP hydrolysis and interference with protein folding in the ER. ER-targeted NTPDase3 may be a useful experimental tool to study the effects of ER ATP depletion on ER function under normal and stress conditions.

The NTPDases are a family of enzymes that hydrolyze nucleoside triphosphates and diphosphates (*1–3*). All these enzymes are similarly synthesized as integral membrane proteins with their active sites located in the lumen of the ER,[1] but differ in their trafficking, being routed to either the ER and Golgi (NTPDases4−7), or to the plasma membrane (NTPDases1−3 and 8). The N-terminal signal sequences of NTPDase5 and 6 can be cleaved, resulting in their release as soluble forms to the outside of the cell. The plasma membrane-localized NTPDases1−3 and 8 are ecto-nucleotidases with similar amino acid sequences and the same membrane topology of two membrane-spanning domains with the catalytic site facing the extracellular milieu. These NTPDases control the concentration of extracellular nucleoside tri- and diphosphates and, thus, modulate signaling via purinergic receptors, which is involved in many physiological processes such as blood clotting, pain perception, and smooth muscle contraction (*1, 3*).

During the folding, trafficking and processing along the secretory pathway, the catalytic sites of NTPDases face the lumen of vesicular compartments where ATP-dependent reactions take place. ATP is transported into ER and Golgi from the cytosol by specific transporters and anion channels (*4, 5*) where it is used as an energy source, a substrate, and a cofactor in a variety of processes, including chaperone-assisted protein folding in the ER (*6–9*) and protein phosphorylation in Golgi (*5, 10, 11*). NTPDases4−7 reside in ER or Golgi, but hydrolyze nucleoside diphosphates and not nucleoside triphosphates, and therefore do not contribute to unproductive hydrolysis of ATP. It is not clear, however, whether the plasma membrane NTPDases1−3 and 8 that only transiently pass through the ER and Golgi are also prevented by some mechanism from hydrolyzing ATP in these compartments.

[†] This work was supported by NIH Grants HL59915 and HL72882 to T.L.K. J.S. was supported by grants from the Canadian Institutes of Health Research (CIHR) and was the recipient of a New Investigator award from the CIHR.

* Address correspondence to this author at Department of Pharmacology and Cell Biophysics, College of Medicine, University of Cincinnati, P.O. Box 670575, Cincinnati, OH 45267-0575. Phone: 513-558-2353. Fax: 513-558-9969. E-mail: terry.kirley@uc.edu.

[‡] University of Cincinnati.

[§] Université Laval.

[1] Abbreviations: ER, endoplasmic reticulum; ERGIC, ER-Golgi intermediate compartment; NEM, *N*-ethylmaleimide; NTPDase3, nucleoside triphosphate diphosphohydrolase 3; NTPDase1, nucleoside triphosphate diphosphohydrolase 1 (also known as CD39); PBS, phosphate-buffered saline.

10.1021/bi800402q CCC: $40.75 
Published on Web 08/12/2008

We initiated this study, in part, based on a previous report (*12*), suggesting that CD39 (also known as NTPDase1) is not active intracellularly and requires terminal glycosylation in the medial- or trans-Golgi compartments for enzyme activity. It was also suggested by Zhong et al. (*12*) that the inactive state of CD39 prior to its arrival to the plasma membrane prevents unproductive hydrolysis of ATP in the secretory pathway and averts potential inhibition of ATP-dependent luminal reactions including protein folding in the ER and phosphorylation in Golgi. We were interested in elucidating the mechanism and subcellular location of NTPDase activation, since this knowledge could potentially provide a novel approach for experimental and therapeutic modulation of NTPDase activity.

Surprisingly, our findings suggest that, in contrast to the reported data for CD39 (*12*), NTPDase3 acquires nucleotidase activity as soon as it is natively folded in the ER or in the ER-Golgi intermediate compartment (ERGIC), and terminal glycosylation in Golgi is not a precondition for the catalytic activity for either NTPDase3, or CD39. In addition, ER-targeted NTPDase3 significantly decreased the efficiency of protein folding, most likely by depleting ATP in ER. These data suggest that a mechanism of spatial separation of highly active nucleotidases from the ATP pool in the ER is likely to function in the secretory pathway to avoid futile hydrolysis of ATP.

## MATERIALS AND METHODS

*DNA Constructs.* The cDNA clone encoding wild-type human NTPDase3 ligated into the pcDNA3 mammalian expression vector was described previously (*13*). The CD39 (NTPDase1) clone was obtained from the same human brain GibcoBRL SuperScript cDNA library using the GibcoBRL cDNA Positive Selection System (*14*). This clone is identical to the published human CD39 DNA sequence (ref *15*, GenBank S73813) in the coding region, except for a G to C silent mutation at position 301. The ER-targeted NTPDase3 construct was made by insertion mutagenesis using the QuikChange II site-directed mutagenesis kit (Stratagene). The sense mutagenesis oligonucleotide encoded the hemagglutinin (HA) epitope (YPYDVPDYA), a spacer (GGGGS), and a C-terminal ER-retention signal (KKLETFKKTN) of a wheat germ agglutinin binding protein 1 (WBP1) (*16*) (see Figure 2A) followed by a stop (TGA) codon. On both flanks of the mutagenesis oligonucleotide, 13−14 bases of the wild-type NTPDase3 cDNA sequence were added to specify the insertion site. Thus, the following sense oligonucleotide was used: 5′-CAGCAACCAGAAggtaccCCTACGACGTGCCCGACTACGCCGGCGGCGGCGGCAGCAAGAAGctcgagACCTTCAAGAAGACCAACTGAAAAGAGGCACTCCG-3′, with the region encoding the HA epitope, the spacer, and the ER retention signal underlined. The *Kpn*I and *Xho*I sites (lower case) were designed within the oligonucleotide to facilitate screening of clones for correct insertion. Wild-type human NTPDase3 DNA was used as a template to produce ER-targeted NTPDase3. In addition, DNA of a catalytically inactive G221A mutant of NTPDase3 (*17*) was used to generate the inactive ER-targeted G221A construct employed as a control. The DNA Core Facility at the University of Cincinnati produced the synthetic oligonucleotides and sequenced all the cDNA constructs to verify the presence of the desired mutations.

*Expression of Recombinant Proteins, Treatment with Monensin and Brefeldin A, and Preparation of COS Cell Membranes.* COS-1 cells were transfected with 4 μg of plasmid DNA per 100 mm plate using Lipofectamine and Plus reagents (Invitrogen). Cotransfection experiments were performed with 3 μg of each of two plasmids. Transfection with an empty pcDNA3 vector was used as a control. Approximately 48 h post-transfection, the COS-1 cells were harvested by scraping in buffer A (30 mM MOPS-NaOH, pH 7.4, 2 mM EDTA, 250 mM sucrose), homogenized, and the crude cell membrane preparations were obtained by centrifugation as described (*13*). In some experiments, 2 mM NEM was added to buffer A in order to prevent the spurious dimerization of NTPDase3 via intermolecular disulfides formed by Cys10, which occur to varying degrees during COS cell membrane preparation under nonreducing conditions (*18*). The presence of 2 mM NEM does not affect the activity of NTPDase3. Monensin (Sigma) and brefeldin A (Sigma) were stored as 10 mM and 10 mg/mL solutions, respectively, in ethanol. Unless stated otherwise, monensin or brefeldin A was added to the cell culture medium to a final concentration of 10 μM or 10 μg/mL, respectively, at 3 h post-transfection and incubated with cells for 24 h, followed by preparation of cell membranes.

*Biotinylation of Cell-Surface Proteins.* Cell-surface proteins were labeled with EZ-Link Sulfo-NHS-LC-Biotin (Pierce) that reacts with primary amino groups, and is impermeable to the plasma membrane. 100 mm plates containing transfected COS-1 cells were placed on ice, washed twice with ice-cold PBS, and then incubated with the biotinylation reagent (0.5 mg/mL in PBS, pH 7.5) for 1 h at 4 °C. The cells were washed with ice-cold PBS and incubated with a quenching buffer (50 mM glycine in PBS) for 10 min at 4 °C. Cells were harvested in buffer A containing 50 mM glycine and processed for cell membrane preparation (*13*). The cell membranes (70 μg) were solubilized with 1% Triton X-100 containing 1 mM EDTA and 1% of Protease Inhibitor Cocktail Set III (Calbiochem) for 20 min at 21 °C, and then centrifuged in an Airfuge for 20 min at 100000*g*. The supernatant was diluted with TBS buffer (150 mM NaCl, 20 mM Tris-HCl, pH 7.3) containing 1% Triton X-100, and incubated with 15 μL of ImmunoPure Immobilized Streptavidin agarose beads (Pierce) for 20 h with end-over-end rotation at 4 °C. Beads were then washed three times with TBS containing 1% Triton X-100, and biotinylated proteins were eluted by resuspending the beads in SDS loading buffer containing 200 mM DTT and boiling for 5 min. Beads were removed by centrifugation, and the supernatant was analyzed by Western blotting.

*Protein Assay.* Protein concentrations were determined using the Bio-Rad protein assay reagent with the modifications of Stoscheck (*19*), using bovine serum albumin as the standard.

*Deglycosylation.* Deglycosylation was performed using Endoglycosidase H (Endo H) or Neuraminidase (New England Biolabs). NTPDases in crude membrane preparations (1 mg/mL) were solubilized with 1% Triton X-100 containing 1 mM EDTA and 1% of Protease Inhibitor Cocktail Set III (Calbiochem) for 15 min at 21 °C, and then

centrifuged in an Airfuge for 20 min at 100000*g*. The supernatant was combined with the appropriate buffer (New England Biolabs) and subjected to deglycosylation according to the manufacturer's instructions by incubation at 37 °C for 1 or 3 h. The same deglycosylation patterns in these samples indicated the completeness of the reaction after 1 h. The controls were incubated under the same conditions, but without glycosidases. The samples were then combined with SDS loading buffer containing 200 mM DTT and analyzed by Western blotting.

*SDS−PAGE and Western Blotting.* Precast 10 or 15 well 4−15% gradient minigels (Bio-Rad) were used for SDS−PAGE. In most experiments, proteins were run in the gels for approximately twice the time needed for the Bromphenol Blue dye to reach the bottom of the gels, in order to improve the resolution in the molecular weight range of the NTPDase proteins. After electrophoresis, the proteins were electrotransferred to Immun-Blot PVDF membrane (Bio-Rad) and processed as described (*20*). NTPDase3 was detected with KLH11 rabbit polyclonal antiserum generated against an internal peptide (amino acid residues 311−327) of human NTPDase3 (*21*). CD39 was detected with KLH3 rabbit polyclonal antiserum raised against the C-terminal sequence of human CD39 (FHKPSYFWKDMV) (*14*). Following an application of a secondary Stabilized Goat Anti-Rabbit HRP-Conjugated antibody, immunoreactivity was detected by chemiluminescence using SuperSignal West Dura Extended Duration Substrate (Pierce), and was recorded using FluorChem IS-8800 system (Alpha Innotech), or Blue Autorad Film (BioExpress). For quantitative estimation of NTPDase proteins in the treated samples as related to control samples, the chemiluminescence intensity of the protein bands was determined using AlphaEaseFC software (Alpha Innotech). The serial dilutions of the control and treated samples were also analyzed on the same immunoblot to generate a standard curve, which was used to estimate protein amounts by chemiluminescence intensities.

*ATPase Assay.* ATPase activity was determined by measuring the amount of inorganic phosphate ($P_i$) released from 0.3 mM ATP in the presence of 5 mM $Ca^{2+}$ at 37 °C using a malachite green procedure (*22*). In all experiments, the values were corrected for the background activity of COS-1 cells transfected with an empty pcDNA3 vector. In some experiments, ATPase activity of NTPDases located on the cell surface was assayed using live cells as follows. COS-1 cells were grown and transfected in 40 mm plates. For ATPase assay, plates were washed twice with an isotonic buffer (140 mM NaCl, 5 mM KCl, 1 mM $CaCl_2$, 20 mM MOPS−NaOH, pH 7.4), 0.8 mL of the buffer was added to each plate, and the plates were placed on a rocking platform at 21 °C. Reaction was initiated by adding 0.2 mL of 12.5 mM ATP in isotonic buffer containing 15 mM $CaCl_2$ to achieve a 2.5 mM final ATP concentration. Inorganic phosphate was assayed in 20 $\mu$L aliquots taken from the plates in 2 min intervals.

*Ion Exchange Chromatography.* Ecto-nucleotidases expressed in COS-1 cells were solubilized by incubation of approximately 1 mg of crude membrane preparation in 1.5 mL of 50 mM Bis-Tris buffer, pH 6.5, containing 2% Protease Inhibitor Cocktail Set III (Calbiochem) and 1% Triton X-100 for 15 min at 21 °C. In some experiments, 2 mM NEM was added to the solubilization buffer in order to prevent the potential disulfide-mediated dimerization of the protein via Cys10 located in the cytoplasmic N-terminus, and Cys501 and Cys509 located in the C-terminal transmembrane domain (*18*). The presence of 2 mM NEM does not affect the activity of NTPDase3, either in the absence or presence of Triton X-100. The sample was centrifuged for 1 h at 100000*g*, and the supernatant was applied onto a 1 mL Bio-Rad High Q anion exchange cartridge (with a trimethyl quaternary amine functional group, $-N^+(CH_3)_3$) equilibrated with buffer B (50 mM Bis-Tris, 0.1% Triton X-100, pH 6.5). Fractions (0.6 mL/min) were collected beginning with washing the cartridge with 3 mL of buffer B, followed by elution with 20 mL of a 0−200 mM NaCl gradient in buffer B, and finally washing with 500 mM NaCl in buffer B. The fractions were assayed for ATPase activity using the malachite green procedure (*22*), and analyzed for the relative amount of the ecto-nucleotidase protein by Western blotting.

*Immunofluorescence Microscopy.* COS-1 cells grown on Laboratory-Tek II chamber glass slides (Nunc) and transfected with the appropriate plasmid cDNA were washed with PBS and fixed with 4% formaldehyde (Ted Pella) in PBS for 20 min at room temperature. Cells were then washed twice with PBS and blocked with buffer C (5% fetal bovine serum, and 0.2% saponin in PBS) overnight at 4 °C. For immunostaining, cells were incubated with 5 $\mu$g/mL monoclonal antibody (IgG produced by hybridoma clone hN3-$H10_s$, specific for human NTPDase3, generated in the laboratory of J.S., manuscript in preparation) in buffer C for 2 h at room temperature, washed twice with buffer C, and incubated with FITC-conjugated goat antimouse IgG (Jackson ImmunoResearch Laboratories) in buffer C (5 $\mu$g/mL) for 1 h at room temperature. The cells were washed with buffer C, rinsed three times with PBS, and mounted in ProLong Gold antifade (Molecular Probes). Samples were viewed and photographed using a Nikon Microphot FXA microscope coupled with a SpotII CCD camera.

## RESULTS

*Glycosylation and Cellular Localization of NTPDase3.* NTPDase3 has 7 potential N-glycosylation sites (*13*). To characterize the localization of the enzyme in the secretory pathway, we analyzed carbohydrate chain modifications that are specific for successive steps of protein trafficking from the site of polypeptide synthesis in the ER to the site of physiological function on the plasma membrane (Figure 1A). The electrophoretic pattern of the wild-type human NTPDase3 expressed in COS-1 cells is represented by two bands: a major broad band of approximately 75 kDa and a faint sharp band of approximately 50 kDa (Figure 1B, lane 1). Deglycosylation with peptide N-glycosidase (PNGase) converts the upper band to the size of the lower band indicating that the lower band represents the nonglycosylated protein core, and the upper band is a fully glycosylated enzyme (see ref *21*). Endo H recognizes and hydrolyzes high-mannose and hybrid, but not complex, N-linked oligosaccharides (*23*). Most proteins remain sensitive to Endo H while they are in ER and in cis- to medial-Golgi, and become Endo H-resistant after they are processed in the medial-Golgi complex (*24*). However, some high-mannose glycans may be masked from terminal glycosylation in Golgi and be present in mature

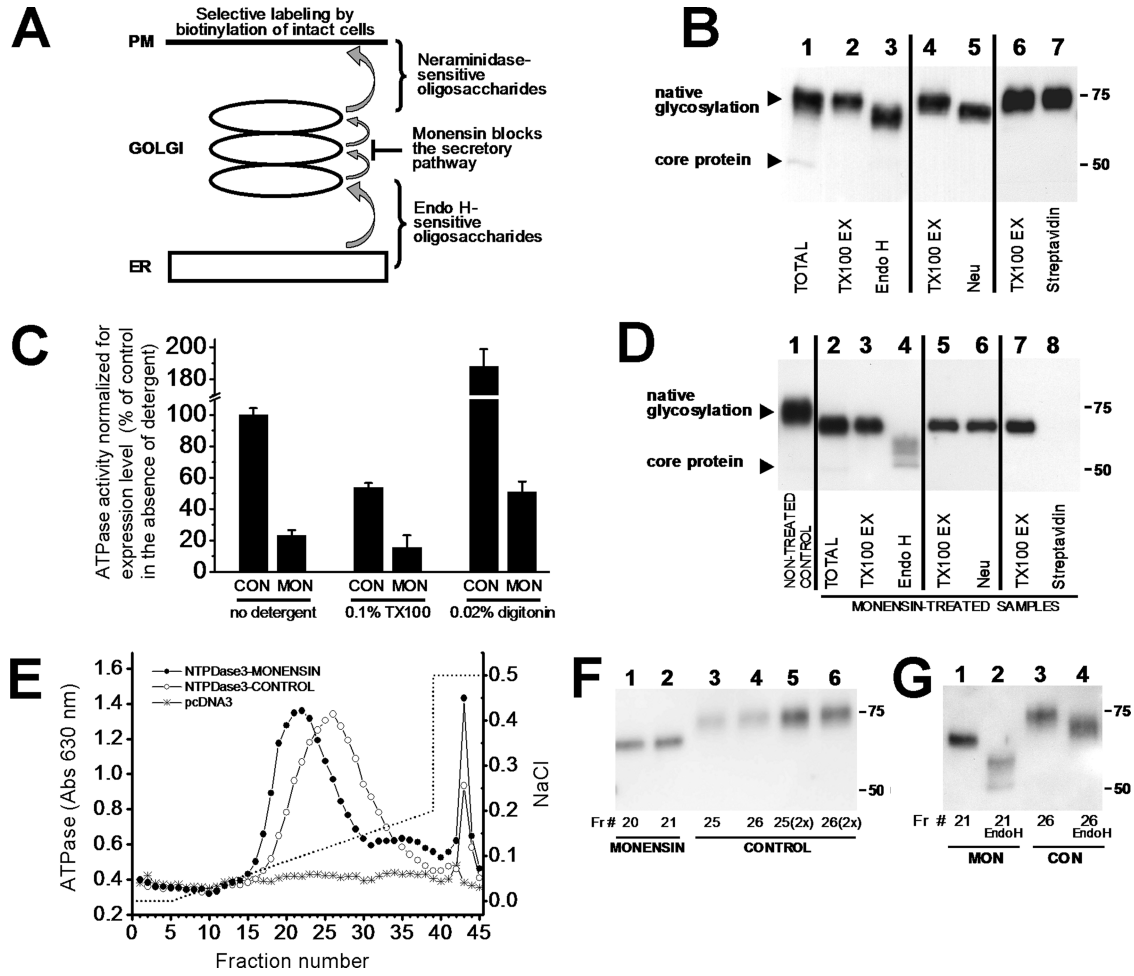


FIGURE 1: Monensin blocks the transport of NTPDase3 to the plasma membrane and causes the intracellular accumulation of catalytically active NTPDase3. Panel A: Schematic explanation of methods used to analyze localization of NTPDase3 molecules. Endo H specifically recognizes and removes the high-mannose N-glycans that are characteristic of immature proteins resident in the ER. Decrease of the molecular mass of the Endo H-treated protein to that of the nonglycosylated core protein indicates ER localization, while a smaller shift in electrophoretic mobility suggests maturation in Golgi. The mature plasma membrane-localized NTPDase3 and CD39 possess at least one high-mannose or hybrid N-glycan, and therefore, show a slight reduction in the apparent molecular mass after treatment with Endo H. Neuraminidase removes sialic acid residues added to N-glycans in the trans-Golgi. Accordingly, the increase in the electrophoretic mobility of neuraminidase-treated protein indicates its processing in trans-Golgi. Biotinylation of intact cells identifies the proteins on the cell surface. Panel B: Glycosylation and localization analysis of NTPDase3 expressed in COS cells. NTPDase3 was solubilized with Triton X-100 (100000*g* supernatant) and subjected to treatment with Endo H (lane 3), or neuraminidase (lane 5). Lanes 1, 2, and 4 are control samples not treated with glycosidases. TOTAL, total sample obtained by dissolving COS membranes directly in SDS loading buffer; TX100 EX, Triton X-100 soluble extract (100000*g* supernatant). The advantage of using Triton X-100 extracts is that they do not contain the nonglycosylated core protein, simplifying the interpretation of electrophoretic patterns after Endo H treatment, which reduces the apparent molecular mass of some bands to that of the core protein. In biotinylation experiments (lanes 6 and 7), intact cells were incubated with the biotinylation reagent, followed by preparation of crude membrane samples. Lane 6 shows NTPDase3 solubilized with Triton X-100 and recovered in 100000*g* supernatant. The supernatant was then incubated with streptavidin beads, and the protein bound and then eluted from beads is shown in lane 7. Panel C: Effect of detergents on ATPase activity of NTPDase3 in crude membrane preparations of COS cells treated with monensin (MON) and nontreated controls (CON). ATPase activity was assayed either in the absence of detergents, or in the presence of 0.1% Triton X-100 or 0.02% digitonin. The graph shows the relative activity of NTPDase3 in samples containing the same amount of immunoreactive NTPDase3 protein, as evaluated by Western blotting. The absolute specific activity of the control sample in the absence of detergent is 300 $\mu$mol of released inorganic phosphate ($P_i$) per h and per mg of crude membrane protein. Due to the 3.5-fold lower expression level of NTPDase3 in monensin-treated samples, specific activity of these samples per mg of crude membrane protein is 3.5 times lower than activity shown in the graph. Values represent means ± SD of three transfections. Panel D: Glycosylation and intracellular localization analysis of NTPDase3 in COS cells treated with monensin. NTPDase3 was solubilized with Triton X-100 (100000*g* supernatant) and subjected to treatment with Endo H (lane 4), or neuraminidase (lane 6). Lanes 2, 3, and 5 are control samples not treated with glycosidases. Following biotinylation of intact cells, NTPDase3 was solubilized with Triton X-100 (lane 7) and incubated with streptavidin beads. Lane 8 shows that no detectable amount of biotinylated NTPDase3 was bound to, and subsequently eluted from, the beads. For comparison, NTPDase3 from control cells (not treated with monensin) is shown in lane 1. Panel E: Ion exchange chromatography of NTPDase3 from transfected monensin-treated (NTPDase3-MONENSIN) or nontreated (NTPDase3-CONTROL) cells, as well as the background of cells transfected with an empty expression vector (pcDNA3). NTPDase3 in 0.8−0.9 mg of crude membrane samples was solubilized with Triton X-100 (100000*g* supernatant) and subjected to chromatography. Due to the approximately 3.5 times lower expression level of NTPDase3 in monensin-treated cells, 5 times larger aliquots were used to assay ATPase activity in the fractions of the monensin-treated sample compared to the nontreated control. The dotted line indicates NaCl concentration in the elution buffer. Panel F: Comparison of specific ATPase activities in the peak fractions of monensin-treated and nontreated samples shown in panel E. The volumes of the peak fractions of monensin-treated and nontreated samples containing the same number of units of ATPase activity were analyzed by Western blotting (lanes 1−4). For comparison, twice the amounts of control fractions were also analyzed in lanes 5 and 6. Note that the densities

FIGURE 1 CONTINUED: of the bands in lanes 1−2 are higher than those in lanes 3−4, but lower than those in lanes 5−6, indicating that the specific ATPase activity of NTPDase3 in the monensin-treated samples corresponds to a value between 50% and 100% (approximately 77% as estimated by densitometry) of the nontreated control. Panel G: Glycosylation analysis of the peak fractions of monensin-treated and nontreated samples shown in panel E. The peak fractions of monensin-treated (MON) and nontreated (CON) samples were digested with Endo H (lanes 2 and 4) and compared to nondigested samples (lanes 1 and 3) by Western blotting using KLH11 antiserum.

glycoproteins (*25*). The latter applies to at least one glycan in wild-type NTPDase3, as the treatment with Endo H slightly reduced the apparent molecular mass to approximately 70 kDa (ref *21*, and Figure 1B, compare lanes 2 and 3) indicating that at least one N-glycosylation site in the mature enzyme is high-mannose or hybrid in structure. However, the shift in electrophoretic mobility is small compared to the position of the nonglycosylated core protein, demonstrating that most of the N-glycosylation sites are processed to complex oligosaccharides, and that the enzyme passed through the medial Golgi compartment. Removal of sialic acids with neuraminidase slightly increases the electrophoretic mobility of the major band (Figure 1B, compare lanes 4 and 5) indicating that NTPDase3 molecules passed through the trans-Golgi and trans-Golgi network (TGN) compartments where the terminal acquisition of sialic acid residues takes place. Finally, accessibility to the extracellularly added, membrane impermeant biotinylation reagent (Figure 1B, compare lanes 6 and 7) identifies the location of the enzyme in the plasma membrane.

The electrophoretic pattern of NTPDase3 indicates a lack of detectable amount of partially glycosylated molecules en route from the ER to the plasma membrane. This molecular pool would be represented in Endo H-treated samples by a spectrum of bands with intermediate electrophoretic mobilities between the core protein of 50 kDa and the mature enzyme treated with Endo H of 70 kDa. This lack of a detectable quantity of the intracellular enzyme at the post-ER stages of secretory pathway makes it impossible to estimate its catalytic activity. Therefore, in order to accumulate an intracellular pool of NTPDase3, we used two approaches: blocking the membrane trafficking with monensin or brefeldin A, and redirecting NTPDases to stay in the ER by addition of a C-terminal dilysine ER retention/retrieval signal.

*Monensin and Brefeldin A Treatment Results in Intracellular Accumulation of Catalytically Active NTPDase3.* Monensin is an ionophore that facilitates the transmembrane exchange of sodium ions for protons (*26*). This causes the neutralization and disruption of acidic intracellular compartments such as the trans-Golgi cisternae. While the response to monensin may vary in different cells (*26*), it generally blocks intracellular transport at the level of mid- or trans-Golgi without significant effect on protein synthesis (*26, 27*). Brefeldin A is a fungal metabolite that disrupts the secretory pathway by blocking the anterograde membrane movement from the ER to the Golgi apparatus, but allows the retrograde transport of membranes from cis/medial-Golgi to the ER (*28*). The glycoproteins retained in the ER in brefeldin A-treated cells were found to undergo processing by cis/medial-Golgi enzymes, but not by trans-Golgi enzymes (*28*).

Treatment with monensin or brefeldin A (data for brefeldin A are similar to those presented for monensin and are therefore not shown) resulted in an accumulation of NTPDase3 molecules with decreased apparent molecular mass of approximately 65 kDa (Figure 1D, lanes 2 and 3) compared to NTPDase3 of 75 kDa from nontreated cells (Figure 1D, lane 1), suggesting incomplete oligosaccharide modification in the Golgi complex. As expected, treatment with Endo H produced a spectrum of bands (Figure 1D, lane 4), thus indicating various degrees of N-glycan maturation. The apparent molecular mass of some molecules was reduced to that of the core protein, suggesting that all N-glycans in these molecules were of high-mannose type characteristic of the ER and sensitive to Endo H (Figure 1D, lane 4). All the enzyme molecules lacked sialic acid residues as demonstrated by their insensitivity to neuraminidase digestion (Figure 1D, lane 6), indicating that they were not exposed to the enzymes of the trans-Golgi compartment. Biotinylation of intact cells failed to label NTPDase3 in monensin-treated cells (Figure 1D, lane 8), in contrast to nontreated control (Figure 1B, lane 7). These results indicate that, in monensin-treated cells, NTPDase3 is localized intracellularly, reaching neither the trans-Golgi nor the plasma membrane.

The complete block of NTPDase3 transport to the plasma membrane with monensin allowed estimation of the enzymatic activity of intracellular NTPDase3 by measuring the total nucleotidase activity in crude membrane samples and subtracting the background of COS cells transfected with an empty pcDNA3 vector (Figure 1C). Because the prolonged (24 h) treatment with monensin decreased the expression level of NTPDase3 (by 3.5 ± 0.7 times as determined by quantitation of chemiluminescence intensity of the protein bands), ATPase activity shown in Figure 1C was normalized to this lower expression level. Intracellular NTPDase3 in monensin-treated cells exhibits 23 ± 3% ATPase activity of nontreated control in the absence of detergent. Addition of Triton X-100 at 0.1% to the reaction mixture reduced ATPase activity approximately 2-fold in control and 1.4-fold in monensin-treated samples (54 ± 3% and 16 ± 8%, respectively), whereas digitonin at 0.02% increased ATPase activity approximately 2-fold in both control and monensin-treated samples (188 ± 11% and 51 ± 7%, respectively), as shown in Figure 1C. The similar inhibitory effect of Triton X-100 on both control and monensin-treated samples indicates that there is no substantial increase in activity due to opening of the intracellular vesicles containing NTPDase3 by detergent. Thus, it seems likely that the numerous large vesicles accumulated in monensin-treated cells are easily ruptured during preparation of crude membrane samples, so that the presence of Triton X-100 does not increase their permeability to ATP. These results demonstrate that intracellular NTPDase3 accumulated in monensin-treated cells is enzymatically active.

Prolonged treatment with monensin and brefeldin A (from 3 h until 27 h after transfection) was used in our experiments for complete block of NTPDase3 transport to the plasma membrane and accumulation of the intracellular enzyme. This protocol, however, is likely to cause ER stress (*29, 30*) and accumulation of misfolded and aggregated NTPDase3 molecules, which can be detected by SDS−PAGE under nonreducing conditions and Western blotting (data not shown). We found that native NTPDase3 can be purified from misfolded aggregates by extraction with Triton X-100

(100000*g* supernatant) and ion exchange chromatography (Figure 1E). For optimal resolution, chromatography was performed at pH 6.5, which is only slightly above the calculated isoelectric point of the human NTPDase3 core protein (p$I$ = 5.98). NTPDase3 is stable in the employed buffer system (50 mM Bis-Tris, 0.1% Triton X-100, pH 6.5), with no detectable decrease in ATPase activity in eluted fractions after overnight storage at 4 °C. NTPDase3 from monensin-treated samples was eluted at lower salt concentration with a remarkable leftward shift of the peak and the right shoulder compared to the enzyme from the control sample (Figure 1E). This shift in elution profile is likely due to the lack of negatively charged sialic acid residues in monensin-treated NTPDase3 samples, thus further supporting the notion that the enzyme did not reach the trans-Golgi compartment.

Specific activity of partially purified NTPDase3 from the monensin-treated sample corresponds to a value between 50% and 100% of the nontreated control, as estimated by Western blot analysis of the amount of NTPDase3 protein in the aliquots exhibiting the same ATPase activity (Figure 1F). This value is noticeably higher than specific activity of approximately 30% assayed in monensin-treated crude membranes in the presence of Triton X-100 (Figure 1C), indicating substantial purification of native NTPDase3 from misfolded molecules. Endo H digestion demonstrates an immature glycosylation pattern of NTPDase3 in the peak chromatographic fractions of the monensin-treated sample (Figure 1G, lane 2) similar to that in the Triton X-100 extract of crude membrane preparation (Figure 1D, lane 4).

Analysis of the subcellular location of NTPDase3 in monensin or brefeldin A-treated cells (data for brefeldin A are similar to those presented for monensin and not shown) strongly suggests that the processing of NTPDase3 was blocked at the level of the Golgi apparatus, and that the enzyme did not reach either the trans-Golgi compartment where sialylation takes place, or the plasma membrane, as demonstrated in cell surface biotinylation experiments. The specific ATPase activity of this intracellular enzyme is approximately 77% of the natively processed NTPDase3 from nontreated control cells (Figure 1F) suggesting that neither glycosylation in trans-Golgi nor delivery to the cell surface is required for nucleotidase activity of NTPDase3.

*ER-Targeted NTPDase3 is Catalytically Active.* In order to investigate the catalytic activity of NTPDase3 at the earliest stages of secretory transport, we attempted to accumulate the enzyme in the ER by redirecting its trafficking with an ER-retention signal. For construction of ER-targeted NTPDase3, we deleted the C-terminal part of the cytosolic tail in the wild-type enzyme which is not necessary for normal processing or activity of NTPDase3 (*31*), and added the ER targeting signal from the wheat germ agglutinin binding protein 1 (WBP1 (*16*)) together with the hemagglutinin (HA) epitope and a spacer (Figure 2A). WBP1 signal sequence contains a dilysine carboxyl-terminal motif (−K(X)KXX), which mediates ER residence via its interaction with the coat protein I (COPI) complex (*32*). The signal-containing proteins are thought to undergo COPI-mediated retrieval from the post-ER compartments, ERGIC and cis-Golgi (*33, 34*). In addition, direct retention of the signal-containing proteins in ER may take place (*35*).

ER-targeted NTPDase3 expressed in COS-1 cells is represented in immunoblots by a major band of approximately 65 kDa, and a minor band of approximately 55 kDa corresponding to the core protein (Figure 2B, lane 1). Treatment with Endo H shifted the electrophoretic mobility of the major band to that of the core protein, indicating that all N-linked oligosaccharides are of the high mannose type characteristic of ER-residing proteins (Figure 2B, lane 3). In contrast, the molecular mass of the wild-type NTPDase3 of 75 kDa (Figure 2B, lane 4) was only slightly decreased after treatment with Endo H (Figure 2B, lane 5) suggesting that at least one of the N-glycosylation sites is high-mannose in structure, whereas the other glycosylation sites are of the complex type. Insensitivity of the ER-targeted NTPDase3 to neuraminidase (Figure 2B, compare lanes 6 and 7) suggests the lack of sialic acid residues, which are characteristic for the mature wild-type enzyme (Figure 2B, compare lanes 8 and 9). As expected, no ER-targeted NTPDase3 was detected on the cell surface in biotinylation assays (Figure 2B, lane 11). All these results, and the deglycosylation analysis with Endo H in particular, revealed no traces of oligosaccharide modification characteristic of the Golgi apparatus, suggesting that ER-targeted NTPDase3 either is retained in the ER or is retrieved back to the ER primarily from the pre-Golgi compartment, ERGIC.

The expression level of ER-targeted NTPDase3 in COS-1 cells was similar to, or slightly higher than, that of the wild-type enzyme, as determined by Western blotting. Consequently, the specific activity of ER-targeted NTPDase3 was compared with that of the wild-type enzyme by measuring ATPase activity in the same protein amount of crude membrane preparations (Figure 2C). ER-targeted NTPDase3 exhibits 6 ± 3% ATPase activity of the wild-type in the absence of detergent. Addition of Triton X-100 to a final concentration of 0.1% in the enzyme assays reduced ATPase activity of the wild-type enzyme approximately 2-fold (53 ± 5%), but, in contrast, increased the activity of ER-targeted NTPDase3 approximately 3.5 times (21 ± 3%), suggesting the intraluminal localization of ER-targeted NTPDase3 (Figure 2C). In contrast to the effect of Triton X-100, digitonin at 0.02% increased ATPase activity of the wild-type enzyme approximately 2-fold (230 ± 20%) and increased the activity of ER-targeted NTPDase3 approximately 4-fold (23 ± 2%) as shown in Figure 2C. Remarkably, the activity of ER-targeted NTPDase3 in the presence of digitonin is approximately the same as in the presence of Triton X-100, whereas the activity of the wild-type enzyme is approximately 4.4 times higher in the presence of digitonin than in the presence of Triton X-100 (Figure 2C). This observation indicates the differences in biochemical properties of the plasma membrane and ER-targeted NTPDase3. The complex effects of digitonin on catalytic activity of NTPDases have been previously documented, but are not well understood (*36*), and likely involve modification of membrane fluidity via modulation of the cholesterol level in membranes, permeabilization of membranes, interaction with the enzyme transmembrane domains, and modification of the oligomerization status of NTPDases. Therefore, while the experiments with digitonin demonstrate the enzymatic activity of ER-targeted NTPDase3, a reliable mechanistic interpretation of the digitonin effect is not possible.

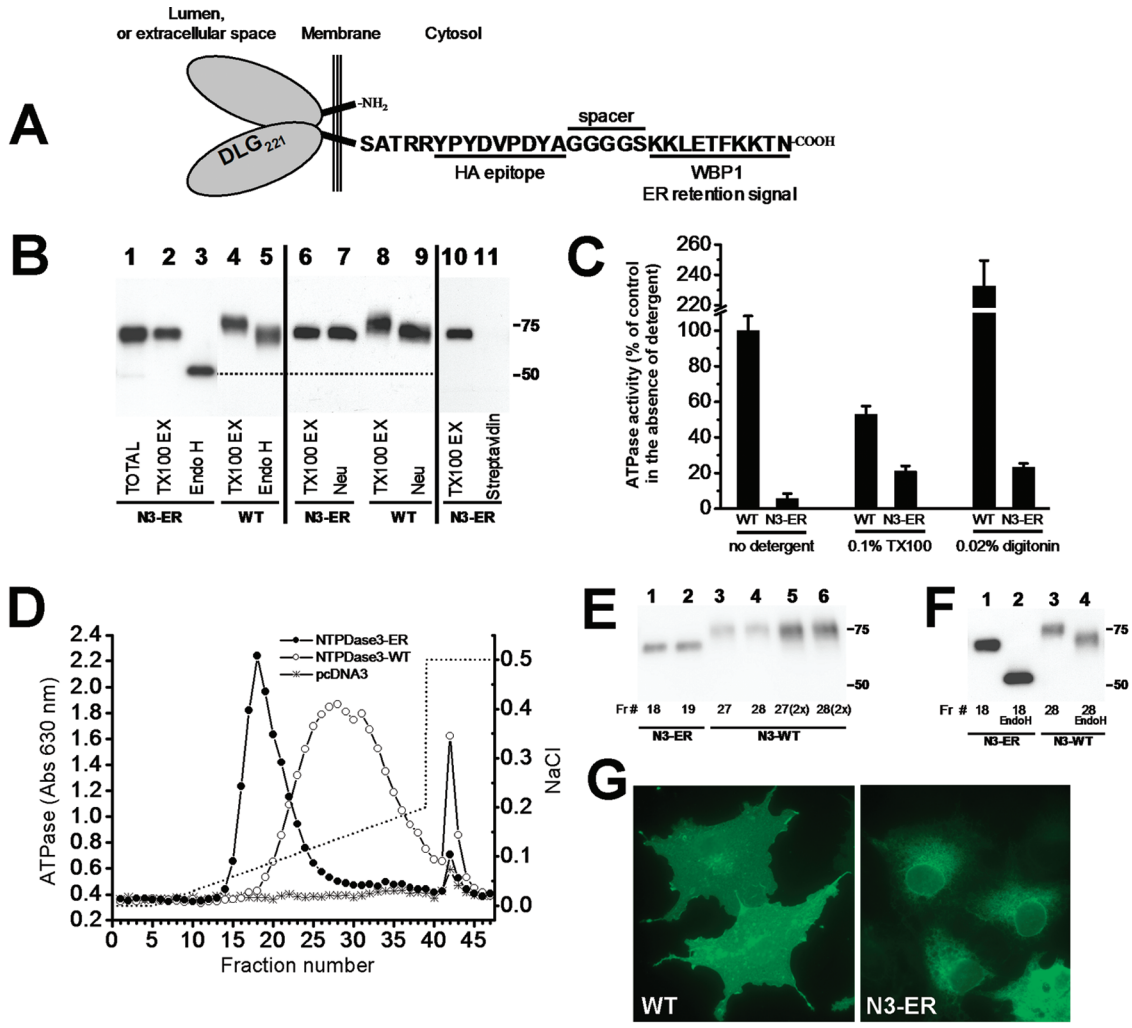


FIGURE 2: ER-targeted NTPDase3 is catalytically active. Panel A: Schematic representation of the construct made for targeting NTPDase3 to ER. The last 15 amino acid residues in the cytosolic C-terminal tail of wild-type NTPDase3 were replaced by 24 amino acid residues containing a HA epitope for potential use in immunofluorescence microscopy, a spacer for the optimal presentation of the retention signal, and the ER retention signal from the wheat germ agglutinin binding protein 1 (WBP1) with two critical lysine residues located two residues away from the C-terminus (*16*). The extracytosolic part of the enzyme containing the active site is represented by two ovals illustrating the two lobes of the NTPDase3 molecular model (*21*). The active site is formed by a cleft between two lobes with ACR1 and ACR4 (apyrase conserved regions) on either side of the cleft. The conservative "$_{219}$DXG$_{221}$" motif in ACR4 is shown in the C-terminal lobe. The G221A mutant used in this study is normally processed, but lacks nucleotidase activity. The active site is exposed to the lumen of ER and other compartments of the secretory pathway, and to the extracellular space after delivery of the enzyme to the plasma membrane. Panel B: Glycosylation and intracellular localization analysis of ER-targeted NTPDase3 expressed in COS cells. ER-targeted NTPDase3 (N3-ER) was solubilized with Triton X-100 (lanes 2, 3, 6, and 7) and treated with Endo H (lane 3), or neuraminidase (lane 7). Lanes 1, 2, and 6 are samples without glycosidase treatment. TOTAL, total sample obtained by dissolving COS membranes directly in SDS loading buffer; TX100 EX, Triton X-100 soluble extract (100000*g* supernatant). For comparison, wild-type enzyme (WT) treated under similar conditions is shown in lanes 4−5 and 8−9. Following biotinylation of COS cells expressing ER-targeted NTPDase3, the enzyme was solubilized with Triton X-100 (lane 10) and incubated with streptavidin beads. Lane 11 shows that no biotinylated protein is bound to and eluted from the beads, indicating that the enzyme does not reach the cell surface. The dotted line indicates the position of the core protein. Panel C: Effect of detergents on ATPase activity of wild-type NTPDase3 (WT) and ER-targeted NTPDase3 (N3-ER) in crude membrane preparations of transfected COS cells. ATPase activity was assayed either in the absence of detergents, or in the presence of 0.1% Triton X-100, or 0.02% digitonin. ATPase activity was not adjusted for the expression level of the enzymes, which was only slightly higher for ER-targeted NTPDase3 compared to wild-type. The specific ATPase activity of the wild-type sample in the absence of detergent is 212 $\mu$mol of released inorganic phosphate ($P_i$) per h and per mg of crude membrane protein. Values represent means ± SD of three transfections. Panel D: Ion exchange chromatography of ER-targeted NTPDase3 (NTPDase3-ER) in comparison with the wild-type NTPDase3 (NTPDase3-WT). The background of COS-1 cells transfected with an empty vector is also shown (pcDNA3). Crude membrane samples (1.0−1.1 mg) were solubilized with Triton X-100 (100000*g* supernatant) and subjected to chromatography. Aliquots of the same volume were used to assay ATPase activity in the fractions of all samples. Panel E: Comparison of specific ATPase activities in the peak fractions of ER-targeted NTPDase3 (N3-ER) and wild-type NTPDase3 (N3-WT) shown in panel D. Volumes of the peak fractions of ER-targeted NTPDase3 and wild-type NTPDase3 containing the same number of units of ATPase activity were subjected to Western blotting (lanes 1−4). For comparison, twice the amounts of wild-type fractions were analyzed in lanes 5 and 6. Note that the density of the bands in lanes 1−2 is higher than that in lanes 3−4, but lower than in lanes 5−6, indicating that the specific ATPase activity of ER-targeted NTPDase3 corresponds to a value between 50% and 100% of the wild-type (approximately 90% as estimated by densitometry). Panel F: Glycosylation analysis of the peak fractions of ER-targeted NTPDase3 and the wild-type shown in panel D. The peak fractions of ER-targeted NTPDase3 (N3-ER) and wild-type NTPDase3 (N3-WT) shown in panel D were either digested with Endo H (lanes 2 and 4) or not treated (lanes 1 and 3), and analyzed by Western blotting. Panel G: Immunofluorescence microscopy of ER-targeted NTPDase3 (N3-ER) and wild-type NTPDase3 (WT) expressed in COS-1 cells. NTPDase3 (left image) and ER targeted NTPDase3 (right image) were visualized in COS cells by immunostaining using an anti-NTPDase3 monoclonal antibody (clone hN3-H10$_s$) and FITC-conjugated secondary antibody. These results are consistent with expression of the wild-type enzyme on the cell surface, and the expression of the ER targeted enzyme in the ER.

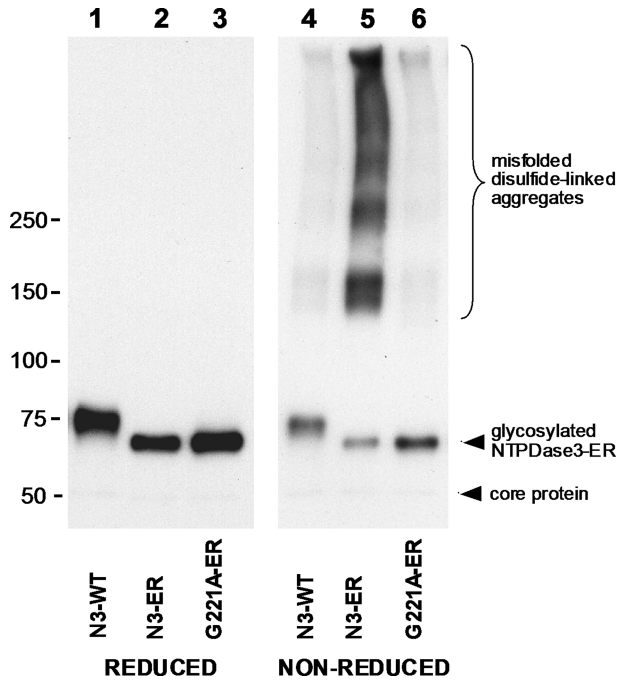


FIGURE 3: Nucleotidase activity of ER-targeted NTPDase3 decreases the efficiency of protein folding in ER. Wild-type NTPDase3 (N3-WT), ER-targeted NTPDase3 (N3-ER) and ER-targeted G221A mutant of NTPDase3 (G221A-ER, which lacks nucleotidase activity) were expressed in COS cells. Crude membranes were prepared in the presence of 2 mM NEM to prevent artificial formation of disulfide-linked dimers and aggregates via oxidation of unpaired cysteines (see Materials and Methods for details) and analyzed by Western blotting under reduced (lanes 1−3) or nonreduced (lanes 4−6) conditions. Immunodetection was performed with the anti-NTPDase3 antibody KLH11. Note that N3-ER sample (lane 5) contains more misfolded, disulfide-linked high molecular mass aggregates than the wild-type (lane 4) or G221A-ER (lane 6) samples. Conversely, the N3-ER sample contains a smaller amount of natively folded enzyme (the band of approximately 65 kDa in lane 5) than G221A-ER (lane 6), indicating a less efficient folding of N3-ER compared to G221A-ER.

Crude membrane samples of ER-targeted NTPDase3 contain significant amounts of misfolded and aggregated molecules (Figure 3, lane 5). In order to accurately evaluate the specific activity of ER-targeted NTPDase3, we purified the active enzyme from misfolded aggregates by extraction with Triton X-100 (100000*g* supernatant) followed by ion exchange chromatography (Figure 2D). ER-targeted NTPDase3 elutes in a relatively narrow peak and at significantly lower ionic strength compared with the broad profile of the wild-type enzyme (Figure 2D). The leftward shift in the elution profile of ER-targeted NTPDase3 is likely due to the lack of the negatively charged sialic acid residues and to the decrease of three units of the net negative charge of the enzyme caused by substitution of the wild-type C-terminal tail with the ER-retention signal and the HA epitope. The sharp elution profile suggests a homogeneous glycosylation pattern of the ER-targeted NTPDase3 compared to the more heterogeneous oligosaccharide structures present in the wild-type enzyme.

Specific activity of purified ER-targeted NTPDase3 corresponds to a value between 50% and 100% (approximately 90% by densitometry) of the wild-type enzyme (Figure 2E). This value is markedly higher than specific activity of approximately 40% assayed in crude membranes in the presence of Triton X-100 (Figure 2C) indicating substantial purification of enzymatically active ER-targeted NTPDase3 away from misfolded molecules. Endo H digestion of the peak chromatographic fractions confirms the high-mannose structure of oligosaccharides in purified ER-targeted NTPDase3, characteristic for proteins residing in the ER (Figure 2F).

Immunofluorescence microscopy reveals an even staining of the wild-type enzyme on the surface of the cells (Figure 2G, left image), and an intracellular reticular network pattern for the ER-targeted NTPDase3 (Figure 2G, right image), which is characteristic for ER-localized proteins. No staining was observed when the primary antibody was omitted, or when the cells were transfected with an empty pcDNA3 vector (data not shown). Collectively, all the results shown in Figure 2 indicate that ER-targeted NTPDase3 is predominantly localized in the ER and that it has not been subjected to detectable processing in the Golgi compartment. The high specific activity of ER-targeted NTPDase3, which is comparable to that of the wild-type NTPDase3, suggests that the enzyme becomes catalytically active in a pre-Golgi compartment, either in the ER or in the ERGIC. Thus, terminal glycosylation in Golgi is not required for the nucleotidase activity of NTPDase3.

*ER-Targeted NTPDase3, but Not ER-Targeted Inactive G221A Mutant, Decreases the Efficiency of Protein Folding.* We attempted to determine whether ER-targeted NTPDase3 exhibits catalytic activity inside the intact ER. Because there are no currently available methods for direct measurement of ATP concentration inside the ER of intact cells, we utilized an indirect approach, in which the nucleotidase activity of ER-targeted NTPDase3 is inferred by estimating the effect of the enzyme on the efficiency of ATP-dependent protein folding in the ER. ATP is delivered from the cytosol into the ER via specific transporters (*4, 37, 38*), and it is assumed that the ATP concentration in the ER lumen is likely to be in the millimolar range, similar to that found in the cytosol (*39*). In the ER, ATP is required for the function of the chaperone proteins for assisting protein folding (*6–9*).

In order to evaluate the effect of the ATPase activity of ER-targeted NTPDase3 on protein folding in the ER, we constructed an ER-targeted, but catalytically inactive, mutant of NTPDase3 (G221A-ER). Gly221 is located in the highly conserved "DXG" phosphate binding motif of the fourth apyrase conserved region (ACR4), which together with ACR1 forms an essential part of the active site of the enzyme (Figure 2A). The G221A mutation does not affect the processing, expression level, or the conformation of NTPDase3, but completely abolishes its enzymatic activity (*17*). We then expressed the ER-targeted NTPDase3, or the catalytically inactive ER-targeted G221A mutant, in COS-1 cells and compared their folding efficiency (Figure 3). The amount of misfolded disulfide-linked aggregates is much higher in samples of enzymatically active ER-targeted NTPDase3 than in samples of inactive ER-targeted G221A mutant, or wild-type (Figure 3, compare lanes 4−6). It should be noted that KLH11 antibody, which was used to probe the Western blot, reacts significantly stronger with dimeric or oligomeric forms than with the monomeric form of NTPDase3, likely due to divalent binding of the antibody to the former versus monovalent binding to the latter. Therefore, the actual ratio of misfolded and natively folded molecules is significantly smaller than the ratio of densities of the

corresponding bands in Figure 3, lanes 4−6. In addition, we also observed that KLH11 antibody reacts markedly stronger with reduced NTPDase3 as compared to the nonreduced protein. Therefore, the density of the bands correlates with the amount of protein when the comparison is made between either reduced (Figure 3, lanes 1−3) or nonreduced (Figure 3, lanes 4−6) samples, but not between reduced and nonreduced samples. The increased amount of misfolded aggregates associated with the expression of active ER-targeted NTPDase3, as compared to inactive ER-targeted G221A mutant, suggests that (1) ER-targeted NTPDase3 is catalytically active *in situ*, i.e. inside the intact ER; (2) the nucleotidase activity of ER-targeted NTPDase3 decreases the efficiency of protein folding; and (3) this decrease in protein folding efficiency is likely due to depletion of ATP in the lumen of the ER. Thus, in these experiments, ER-targeted enzymes were used both as modulators of ATP levels in ER and as reporters of folding efficiency. The low background of misfolded aggregates in the wild-type sample (Figure 3, lane 4) suggests that wild-type NTPDase3 does not substantially affect ATP concentration in ER.

*ER-Targeted NTPDase3 Decreases the Folding Efficiency and the Transport to the Plasma Membrane of the Co-Expressed CD39 Used as a Reporter.* To develop a more sensitive and quantitative assay of protein folding efficiency in ER, we took advantage of a distinct expression pattern of human CD39 (Figure 4A). Unlike human NTPDase3, wild-type human CD39 expressed in COS-1 cells is represented by three bands: a major broad band of approximately 75 kDa, a band of approximately 65 kDa, and a faint sharp band of approximately 50 kDa corresponding to the nonglycosylated core protein (Figure 4A, lane 1). The upper band of 75 kDa has the properties of the mature and completely processed enzyme: its apparent molecular mass is only slightly reduced after deglycosylation with Endo H (Figure 4A, compare lanes 2 and 3), similar to that of the mature NTPDase3 protein (Figure 1B, compare lanes 2 and 3), indicating that at least one N-glycosylation site is high-mannose or hybrid in structure. As expected for the mature enzyme, the protein in upper band is sensitive to neuraminidase hydrolysis (Figure 4A, compare lanes 4 and 5) and accessible to the extracellularly added biotinylation reagent (Figure 4A, compare lanes 6 and 7), demonstrating acquisition of sialic acid residues in the trans-Golgi compartment and localization in the plasma membrane, respectively. The CD39 molecules comprising the lower band of 65 kDa have the properties of an immature protein resident in the ER, since their apparent mass is reduced to that of the core protein after treatment with Endo H (Figure 4A, compare lanes 2 and 3). Consistent with this observation are the lack of effect of neuraminidase treatment (Figure 4A, compare lanes 4 and 5) and the lack of cell-surface biotinylation (Figure 4A, compare lanes 6 and 7). In addition, analysis of CD39 by electrophoresis under nonreducing conditions demonstrates the appearance of high molecular mass aggregates and a decrease in density of the 65 kDa lower band (Figure 4B, compare lanes 1 and 2), suggesting that this band represents misfolded, disulfide-linked aggregated molecules. Collectively, these data characterize the protein in the upper 75 kDa band as mature CD39 located at the plasma membrane, and the protein in the lower 65 kDa band as the misfolded and aggregated molecules retained in the ER.

The presence of both natively folded and misfolded molecules in the samples of CD39 expressed in COS cells prompted us to use CD39 as a reporter of protein folding efficiency in the ER. Any factors that obstruct protein folding in the ER are likely to increase the ratio between the amount of misfolded and natively folded molecules, thus making human CD39 a sensitive indicator of folding effectiveness in the ER. In addition, since the misfolded molecules are retained in ER by a quality control mechanism, only the natively folded enzyme reaches the plasma membrane. Consequently, a simple determination of CD39 nucleotidase activity should be a convenient and quantitative assay for protein folding efficiency in the ER. To test this, we coexpressed CD39 with either active ER-targeted NTPDase3, or inactive ER-targeted G221A NTPDase3 (Figure 4C). As additional controls, CD39 was coexpressed with wild-type (nontargeted) NTPDase3, as well as with the nontargeted inactive G221A mutant of NTPDase3. As schematically shown in Figure 4C, we anticipated that nucleotidase activity of active ER-targeted NTPDase3 (NTPDase3-ER), but not inactive ER-targeted G221A (G221A-ER), would decrease ATP concentration in ER and thus reduce the folding efficiency of CD39 which serves as a reporter protein. Consequently, less natively folded CD39 would reach the plasma membrane resulting in diminished enzymatic activity in cells expressing NTPDase3-ER compared to cell expressing the inactive G221A-ER. Indeed, we found that the total ATPase activity in membrane preparations of cells cotransfected with CD39 and ER-targeted NTPDase3 was approximately 2-fold lower (49 ± 7%) than that in crude membrane samples of cells cotransfected with CD39 and ER-targeted G221A mutant (Figure 4D). The actual CD39 activity in the sample (CD39 + NTPDase3-ER) is slightly lower than 49 ± 7% due to a minor contribution of NTPDase3-ER activity. In order to exclusively analyze cell-surface CD39 activity, we performed assays of live cells attached to culture plates, as described in Materials and Methods. Thus, in five replicated assays, the cell-surface ATPase activity of cells cotransfected with CD39 plus NTPDase3-ER was 46 ± 6% of that measured on cells cotransfected with CD39 plus inactive G221A-ER. These results indicate that ER-targeted NTPDase3 significantly decreases the amount of coexpressed CD39 molecules that attain native folding and reach the plasma membrane.

Western blotting analysis using an anti-CD39 primary antibody also demonstrates a significant increase in the ratio of misfolded (immature glycosylation) to natively folded molecules in cells containing NTPDase3-ER (Figure 4E, lane 3) compared to cells coexpressing inactive G221A-ER (Figure 4E, lane 4). These results demonstrate the inhibitory effect of nucleotidase activity of ER-targeted NTPDase3 on protein folding of coexpressed CD39. The nontargeted enzymes, wild-type and G221A inactive mutant NTPDase3, showed no detectable effect on the folding of the coexpressed CD39 (Figure 4E, lanes 1 and 2). Immunoblotting using an anti-NTPDase3 antibody reveals that the expression level of wild-type NTPDase3 is similar to that of the G221A mutant (Figure 4F, lanes 1 and 2), and that the expression level of NTPDase3-ER is similar to that of G221A-ER (Figure 4F, lanes 3 and 4). These results suggest a significant depletion of ATP in ER by ER-targeted NTPDase3, and demonstrate

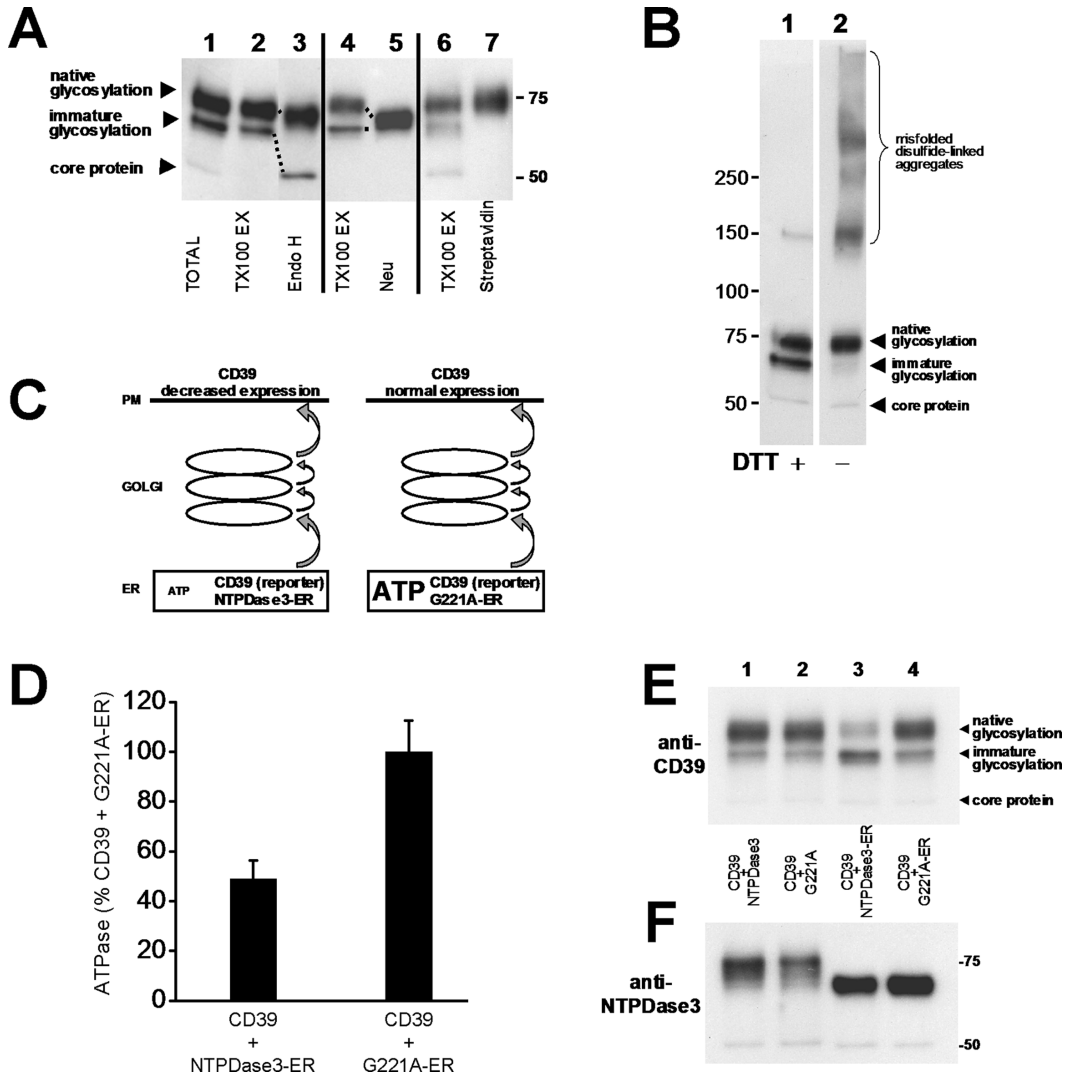


FIGURE 4: ER-targeted NTPDase3 reduces the efficiency of folding and decreases the transport to the cell surface of the coexpressed CD39 used as a reporter protein. Panel A: Characterization of the glycosylation pattern and subcellular localization of CD39 expressed in COS-1 cells. Human CD39 was solubilized with Triton X-100 (100000*g* supernatant) and treated with Endo H (lane 3), or neuraminidase (lane 5). Lanes 1, 2, and 4 are control samples not treated with glycosidases. TOTAL, total sample obtained by dissolving COS membranes directly in SDS loading buffer; TX100 EX, Triton X-100 soluble extract (100000*g* supernatant). Following biotinylation of intact cells, CD39 was solubilized with Triton X-100 (lane 6) and incubated with streptavidin beads. Lane 7 shows that only the molecules in the upper band are biotinylated, indicating their localization on the cell surface. Panel B: CD39 subjected to SDS−PAGE under reducing (lane 1) or nonreducing (lane 2) conditions and analyzed by Western blotting. Note the appearance of high molecular mass aggregates and the decrease in density of the 65kDa band (immature glycosylated protein) under nonreducing conditions, indicating that these aggregates are formed by misfolded and disulfide-linked 65 kDa molecules. Panel C: Schematic representation of the experimental approach to examine the effect of ER-targeted NTPDase3 on protein folding in the ER using CD39 as a reporter protein. ER-targeted NTPDase3 (NTPDase3-ER) or ER-targeted G221A inactive mutant of NTPDase3 (G221A-ER) were expressed in COS cells. If NTPDase3-ER is catalytically active *in situ*, it would likely reduce the ATP concentration in ER and thus decrease protein folding efficiency in ER, while the inactive G221A-ER would not. Wild-type human CD39 is coexpressed and used as a reporter protein in these experiments. Since misfolded molecules represent a substantial portion of CD39 under normal expression in COS cells, the ratio between the natively folded and misfolded molecules (represented by the upper and the lower bands in panel A, lane 1, respectively) should be sensitive to changes in protein folding efficiency. Because only natively folded CD39 molecules are delivered to the cell surface, a reduction in protein folding efficiency should decrease the expression level of CD39 at the plasma membrane, which can be conveniently assayed by measuring CD39 activity. Panel D: ATPase activity of CD39 coexpressed with either ER-targeted NTPDase3 (NTPDase3-ER), or ER-targeted G221A (G221A-ER). ATPase activity was measured in crude membrane preparations of transfected COS cells. The specific ATPase activity of CD39 + G221A-ER sample is 148 $\mu$mol of released inorganic phosphate ($P_i$) per h and per mg of crude membrane protein. Values represent means ± SD of three transfections. Panel E: Western blotting of CD39 coexpressed with one of the following constructs: wild-type NTPDase3 (lane 1), G221A (lane 2), ER-targeted NTPDase3 (lane 3), and ER-targeted G221A (lane 4). Crude membrane samples were subjected to SDS−PAGE under reducing conditions and analyzed by Western blotting using anti-CD39 antibody KLH3. Panel F: Western blotting of the same samples as in panel E, but probed with anti-NTPDase3 antibody KLH11.

the validity of human CD39 as a reporter of protein folding efficiency in ER. In addition, these data suggest that even under conditions of overexpression in COS cells, nontargeted wild-type NTPDase3 is not likely to substantially deplete ATP in ER and affect protein folding.

## DISCUSSION

Characterization of intracellular NTPDase molecules that are on the way from the ER to the plasma membrane is complicated by the steady-state distribution of the enzyme

in three molecular pools: (1) a pool of ER-retained molecules that either did not complete folding (unfolded), or failed correct folding (misfolded) and are likely to be degraded; (2) a pool of correctly folded molecules that left ER, but did not reach the plasma membrane; (3) a large pool of completely processed molecules that reached the site of their physiological function and reside in the plasma membrane. In order to achieve our goal to characterize the molecules in the second pool, we used the following strategy: (i) increase the amount of molecules in the second pool by blocking their trafficking to the plasma membrane; (ii) minimize or eliminate the third molecular pool by continuous exposure to trafficking inhibitors; (iii) separate the second pool from the first and the third pools using ion exchange chromatography.

Accordingly, we applied trafficking inhibitors, monensin or brefeldin A, during the whole period of NTPDase3 expression from 3 to 27 h post-transfection. While the long exposure to trafficking inhibitors likely caused toxic effects in cells and reduced the expression level of the enzyme, it completely prevented the transport of NTPDase3 to the plasma membrane, thus greatly facilitating the analysis of the intracellular enzyme. Our results indicate that monensin and brefeldin A blocked NTPDase3 processing at the level of medial-Golgi. After separation from misfolded molecules by Triton X-100 extraction and ion exchange chromatography, the intracellular NTPDase3 from monensin- or brefeldin A-treated cells demonstrated specific activity similar to that of plasma membrane-located NTPDase3 from nontreated cells, indicating that NTPDase3 acquired enzymatic activity between the ER and the trans-Golgi.

To further delineate the location of NTPDase3 activation, we redirected the enzyme to reside in the ER, instead of being transported to the plasma membrane, by using a dilysine ER retention/retrieval C-terminal signal peptide. Correctly folded ER-targeted NTPDase3 is likely to exit ER in COPII vesicles and then to be retrieved to ER from ERGIC or cis-Golgi compartment in vesicles bearing the protein coat COPI, which recognizes the retrieval signal (*32*). The lack of Golgi-specific carbohydrate modifications in ER-targeted NTPDase3 suggests that the enzyme is retrieved primarily from ERGIC, rather than the cis-Golgi. The possibility that ER-targeted NTPDase3 does not exit ER, but is rather directly retained via the dilysine targeting signal, cannot be excluded (*35*). Specific activity of ER-targeted NTPDase3 separated from misfolded molecules by Triton X-100 extraction and ion exchange chromatography is comparable to that of the mature wild-type enzyme located at the plasma membrane (Figure 2E), indicating that the enzyme becomes active either in the ER or in the ERGIC. Furthermore, ER-targeted NTPDase3 decreases its own folding efficiency (Figure 3), and suppresses the folding and transport to the cell surface of coexpressed CD39 (Figure 4), suggesting that the enzyme is active *in situ*, i.e. inside the intact ER.

We found CD39 to be a useful reporter of protein folding efficiency in the ER. However, coexpression of CD39 with a structurally similar NTPDase3 raises a question of whether potential hetero-oligomerization of these proteins could affect the interpretation of results. While such hetero-oligomerization cannot be excluded, it is unlikely to alter the major conclusion that ER-targeted NTPDase3 depletes ATP level in ER and diminishes the folding efficiency of the coexpressed CD39, for the following reasons. First, only enzymatically active ER-targeted NTPDase3, but not inactive ER-targeted G221A mutant, increases misfolding of CD39 (Figure 4E, compare lanes 3 and 4). Since G221A mutation is located in the active site cleft, and does not affect the expression level and processing of NTPDase3, it is very unlikely to affect the oligomerization capability of the enzyme. Consequently, both ER-targeted NTPDase3 and ER-targeted G221A mutant are likely to equally participate in any potential hetero-oligomerization with CD39. This suggests that it is the ATPase activity of ER-targeted NTPDase3 that causes misfolding of the reporter protein CD39. Second, wild-type NTPDase3 does not affect folding of the coexpressed CD39 (Figure 4E, compare lanes 1 and 3), although it is likely to participate in any potential hetero-oligomerization with coexpressed CD39 in the same way as ER-targeted NTPDase3. This also indicates that it is the ATPase activity of ER-targeted NTPDase3, and the resulting depletion of ATP in the ER, that causes misfolding of the coexpressed CD39.

Our findings raise the question as to how the cell avoids futile hydrolysis of ATP in the secretory pathway while expressing an active ATPase inside the lumen of secretory compartments. Although ER-targeted NTPDase3 has negative effects on protein folding in ER and processing (Figure 3, Figure 4D, and Figure 4E, compare lanes 3 and 4), expression of the wild-type NTPDase3 does not affect the folding of the coexpressed CD39 (Figure 4E, compare lanes 1 and 2). This suggests that, even under conditions of experimental overexpression, wild-type NTPDase3 is not likely to substantially deplete ATP in ER. Considering the high catalytic efficiency ($k_{cat}/K_m$) typical for NTPDases (*40*), this result is somewhat surprising. One possible explanation could be that the steady-state concentration of the catalytically active wild-type NTPDase3 in the ER is low due to rapid export from the ER, so that unproductive hydrolysis of ATP is minimized and compensated for by supplying ATP from the cytosol via ATP transporters, whereas the high protein concentration and ATPase activity of ER-targeted NTPDase3 exceeds the ER ATP supply. Another possibility, which seems more likely, is that wild-type NTPDase3 completes folding and acquires nucleotidase activity in the post-ER, but pre-Golgi, ERGIC compartment. In this scenario, wild-type NTPDase3 is not active inside the ER and does not hydrolyze ATP. In contrast, ER-targeted NTPDase3 is enzymatically active in the ER because it completed native folding and acquired catalytic activity in ERGIC before it was retrieved to ER via interaction of the cytosolic dilysine signal with COPI complex (*32*).

The data presented here suggest that NTPDase3 acquires enzymatic activity as soon as it is natively folded in the ER or in a pre-Golgi compartment, ERGIC. Why do our conclusions contrast with the statements made by Zhong et al. (*12*) that a closely related member of the plasma membrane ecto-nucleotidases, CD39 (NTPDase1), is not active intracellularly, and that only a fully glycosylated and cell surface localized CD39 has nucleotidase activity? Considering the very similar primary structure, topology, and plasma membrane localization of NTPDase3 and CD39, it seems unlikely that they would differ radically in posttranslational processing. As discussed above, our study of a steady-state distribution of NTPDase3 in COS-1 cells revealed no detectable amount of intracellular molecules en

route from ER to the plasma membrane, which made it impossible to measure activity of the intracellular enzyme, if no measures were taken for its accumulation. If the same was true for the rat CD39 expressed in COS-7 cells used by Zhong et al., then the subcellular fractionation of COS-7 cells transfected with CD39 cDNA performed by these authors for the purpose of correlating the distribution of rat CD39 activity and CD39 protein with the distribution of intracellular organelles (Figure 1 from ref *12*) can be interpreted differently for the following reason. We found that a substantial portion of human CD39 expressed in COS-1 cells fails to natively fold and is represented in immunoblots by a protein band with a slightly higher electrophoretic mobility compared to the natively folded enzyme (Figure 4A). The protein in this band is not labeled during biotinylation of intact cells (Figure 4A, compare lanes 6 and 7) and consists of misfolded and aggregated molecules (Figure 4B) retained in ER by the quality control mechanism, as evident by sensitivity to Endo H (Figure 4A, compare lanes 2 and 3). The explanation for this aberrant folding characteristic of human CD39 (NTPDase1) in COS-1 cells, but not of human NTPDase3, is unknown. However, some other proteins also exhibit inefficient processing. For example, only 25% of newly synthesized wild-type cystic fibrosis transmembrane conductance regulator (CFTR) molecules enter post-ER compartments and acquire complex oligosaccharides (*41*). Thus, it seems likely that the rat CD39 expressed in COS-7 cells and used by Zhong et al. also contained a substantial amount of misfolded protein. This is supported by the data in Figure 7A from that study (*12*), where Western blots revealed that rat CD39 expressed in COS-7 cells was represented by two bands, of which only the upper band was accessible for cell surface biotinylation, similar to the expression and biotinylation pattern that we described for human CD39 expressed in COS-1 cells (Figure 4A). Therefore, it is likely that the protein in the lower band in the rat CD39 samples described by Zhong et al. consisted of misfolded and aggregated molecules retained in the ER by the quality control mechanism. Consequently, the subcellular fractionation in a sucrose gradient performed in that work (*12*) did demonstrate the colocalization of the natively folded enzymatically active molecules with the plasma membrane marker, and the misfolded inactive CD39 protein with the ER marker, but did not provide information as to what stage along the secretory pathway the natively folded molecules acquire catalytic activity.

To evaluate the catalytic activity of intracellular human CD39, we attempted to accumulate the enzyme en route from the ER to the plasma membrane using the trafficking inhibitors, monensin and brefeldin A, and the dilysine ER retention signal, following protocols very similar to those described above for NTPDase3. We found that treatment with monensin or brefeldin A for 16 h (from 32 h post-transfection till 48 h post-transfection) resulted in an accumulation of partially glycosylated molecules, which can be separated from the fully glycosylated molecules by ion exchange chromatography in the presence of 0.1% Triton X-100, and which exhibit specific ATPase activity comparable to that of the fully glycosylated enzyme (data not shown). However, continuous exposure to monensin or brefeldin A for 24 h (from 3 h post-transfection till 27 h post-transfection) produced mainly inactive CD39, likely due to drug-induced exaggerated misfolding, which is characteristic for CD39 (data not shown).

In order to investigate the catalytic activity of CD39 at the earliest stages of secretory transport, we constructed and evaluated an ER-targeted human CD39 (see Supporting Information). ER-targeted CD39 expressed in COS-1 cells was represented mainly by denatured and aggregated protein. However, when the correctly folded ER-targeted CD39 was separated from misfolded and aggregated molecules by extraction with Triton X-100 and ion exchange chromatography, the specific activity of ER-targeted CD39 was estimated to be approximately 84% of wild-type CD39 (Supporting Information, Figure S1). These data suggest that, similar to NTPDase3, CD39 does not require terminal glycosylation in Golgi or delivery to the plasma membrane for nucleotidase activity, and that CD39 becomes catalytically active at a pre-Golgi stage of secretory pathway. However, CD39 differs from NTPDase3 since it has an increased propensity for misfolding, which is aggravated by the treatment with trafficking inhibitors, monensin or brefeldin A, or by retargeting the enzyme to ER with an ER-retention signal. This makes it difficult, or impossible, to evaluate the catalytic activity of the intracellular CD39 without prior separation of the natively folded enzyme from the misfolded molecules. Taken together, our results strongly suggest that human CD39 acquires catalytic activity at a pre-Golgi stage of the secretory pathway similar to NTPDase3.

While the extent of ATP depletion in ER which can be achieved by using ER-targeted NTPDase3 remains to be determined, this enzyme construct suggests potential applications beyond NTPDase trafficking. We propose that ER-targeted NTPDase3 may be a useful tool to study the effects of ATP depletion specifically in ER on ER function under normal and stress conditions. The role of ATP in the function of the protein folding machinery in the ER has been intensively investigated in both *in vitro* and *in vivo* systems (*8, 9, 39, 42*). A widely used approach to deplete ATP in the ER of living cells is to inhibit ATP production in whole cells with metabolic poisons that block glycolysis and oxidative phosphorylation (*7, 43, 44*). While this approach has elucidated important properties of ER-located chaperones and other enzymes essential for protein folding, cytotoxicity and potential indirect effects of ATP depletion in the whole cell on protein folding in the ER limit its application and the interpretation of obtained results. ER-targeted NTPDase3 developed here may circumvent some of these side effects, and therefore be a novel tool for depleting ATP specifically in the ER compartment, although its utility requires further investigation.

ER-targeted NTPDase3 may also be instrumental to study the effect of ATP depletion in the ER on endoplasmic reticulum stress response. Various physiological and pathological conditions perturb ER function and homeostasis resulting in an accumulation in the ER of unfolded and misfolded proteins. Under this condition, known as "ER stress", cells activate specific signaling pathways referred to as the unfolded protein response (UPR). The UPR signaling cascades attempt to restore a favorable environment for protein folding in the ER. However, a severe and chronic impairment of ER function may activate a programmed cell death pathway. Consequently, the outcome of the UPR depends on the balance between pro-survival and pro-

apoptotic signaling (*45*). Survival of cancer cells and their resistance to therapeutic drugs have been correlated with overexpression of the major ATP-dependent ER chaperones, GRP78 and GRP94, which enhance the protein-folding capacity in ER (*46, 47*). Accordingly, the inhibition of expression and/or function of these chaperones in cancer cells has been proposed as an approach to activate the apoptotic response and enhance the efficacy of chemotherapeutic drugs (*46–50*). We suggest that an additional approach to inhibit the function of GRP78 and GRP94 is to specifically deplete ER of ATP, and that ER-targeted NTPDase3 should be a useful tool to test this, and other related hypotheses. Although ER-targeted NTPDase3 cannot be used itself as an anticancer agent, a favorable outcome derived from experiments coupling ER-targeted NTPDase3 expression with antineoplastic drug treatment would support the hypothesis that ATP transporters in the ER could be anticancer targets.

## ACKNOWLEDGMENT

We thank Dr. Blanche Schwappach, Zentrum für Molekulare Biologie der Universität Heidelberg (ZMBH), Germany, and Dr. Min Li, Johns Hopkins University School of Medicine, for their advice regarding design of the ER-targeted NTPDase3 and CD39 constructs.

## SUPPORTING INFORMATION AVAILABLE

Construction and characterization of ER-targeted human CD39 (NTPDase1). This material is available free of charge via the Internet at http://pubs.acs.org.

## REFERENCES

1. Robson, S. C., Sévigny, J., and Zimmermann, H. (2006) The E-NTPDase family of ecto-nucleotidases: Structure, function, relationships and pathophysiological significance. *Purinergic Signal. 2*, 409–430.
2. Zimmermann, H. (1999) Two novel families of ectonucleotidases: molecular structures, catalytic properties and a search for function. *Trends Pharmacol. Sci. 20*, 231–236.
3. Plesner, L. (1995) Ecto-ATPases: Identities and functions. *Int. Rev. Cytol. 158*, 141–214.
4. Hirschberg, C. B., Robbins, P. W., and Abeijon, C. (1998) Transporters of nucleotide sugars, ATP, and nucleotide sulfate in the endoplasmic reticulum and Golgi apparatus. *Annu. Rev. Biochem. 67*, 49–69.
5. Thompson, R. J., Akana, H. C., Finnigan, C., Howell, K. E., and Caldwell, J. H. (2006) Anion channels transport ATP into the Golgi lumen. *Am. J. Physiol. Cell Physiol. 290*, C499−514.
6. Dorner, A. J., Wasley, L. C., and Kaufman, R. J. (1990) Protein dissociation from GRP78 and secretion are blocked by depletion of cellular ATP levels. *Proc. Natl. Acad. Sci. U.S.A. 87*, 7429–7432.
7. Braakman, I., Helenius, J., and Helenius, A. (1992) Role of ATP and disulphide bonds during protein folding in the endoplasmic reticulum. *Nature 356*, 260–262.
8. Williams, D. B. (2006) Beyond lectins: the calnexin/calreticulin chaperone system of the endoplasmic reticulum. *J. Cell. Sci. 119*, 615–623.
9. Dollins, D. E., Warren, J. J., Immormino, R. M., and Gewirth, D. T. (2007) Structures of GRP94-nucleotide complexes reveal mechanistic differences between the hsp90 chaperones. *Mol. Cell 28*, 41–56.
10. West, D. W., and Clegg, R. A. (1984) Casein kinase activity in rat mammary gland Golgi vesicles. Demonstration of latency and requirement for a transmembrane ATP carrier. *Biochem. J. 219*, 181–187.
11. Lasa, M., Marin, O., and Pinna, L. A. (1997) Rat liver Golgi apparatus contains a protein kinase similar to the casein kinase of lactating mammary gland. *Eur. J. Biochem. 243*, 719–725.
12. Zhong, X., Malhotra, R., Woodruff, R., and Guidotti, G. (2001) Mammalian plasma membrane ecto-nucleoside triphosphate diphosphohydrolase 1, CD39, is not active intracellularly. The N-glycosylation state of CD39 correlates with surface activity and localization. *J. Biol. Chem. 276*, 41518–41525.
13. Smith, T. M., and Kirley, T. L. (1998) Cloning, sequencing, and expression of a human brain ecto-apyrase related to both the ecto-ATPases and CD39 ecto-apyrases. *Biochim. Biophys. Acta 1386*, 65–78.
14. Hicks-Berger, C. A., and Kirley, T. L. (2000) Expression and characterization of human ecto-ATPase and chimeras with CD39 ecto-apyrase. *IUBMB Life 50*, 43–50.
15. Maliszewski, C. R., Delespesse, G. J., Schoenborn, M. A., Armitage, R. J., Fanslow, W. C., Nakajima, T., Baker, E., Sutherland, G. R., Poindexter, K., Birks, C., Alpert, A., Friend, D., Gimpel, S. D., and Gayle, R. B. I. (1994) The CD39 lymphoid cell activation antigen. Molecular cloning and structural characterization. *J. Immunol. 153*, 3574–3583.
16. Shikano, S., and Li, M. (2003) Membrane receptor trafficking: evidence of proximal and distal zones conferred by two independent endoplasmic reticulum localization signals. *Proc. Natl. Acad. Sci. U.S.A. 100*, 5783–5788.
17. Smith, T. M., and Kirley, T. L. (1999) Site-directed mutagenesis of a human brain ecto-apyrase: Evidence that the E-type ATPases are related to the Actin/heat shock 70/sugar kinase superfamily. *Biochemistry 38*, 321–328.
18. Murphy, D. M., Ivanenkov, V. V., and Kirley, T. L. (2002) Identification of cysteine residues responsible for oxidative cross-linking and chemical inhibition of human nucleoside triphosphate diphosphohydrolase 3. *J. Biol. Chem. 277*, 6162–6169.
19. Stoscheck, C. M. (1990) Increased uniformity in the response of the coomassie blue G protein assay to different proteins. *Anal. Biochem. 184*, 111–116.
20. Smith, T. M., and Kirley, T. L. (1999) Glycosylation is essential for functional expression of a human brain ecto-apyrase. *Biochemistry 38*, 1509–1516.
21. Ivanenkov, V. V., Meller, J., and Kirley, T. L. (2005) Characterization of disulfide bonds in human nucleoside triphosphate diphosphohydrolase 3 (NTPDase3): Implications for NTPDase structural modeling. *Biochemistry 44*, 8998–9012.
22. Baykov, A. A., Evtushenko, O. A., and Avaeva, S. M. (1988) A malachite green procedure for orthophosphate determination and its use in alkaline phosphatase-based enzyme immunoassay. *Anal. Biochem. 171*, 266–270.
23. Maley, F., Trimble, R. B., Tarentino, A. L., and Plummer, T. H., Jr. (1989) Characterization of glycoproteins and their associated oligosaccharides through the use of endoglycosidases. *Anal. Biochem. 180*, 195–204.
24. Freeze, H. H. (1999) Use of glycosidases to study protein trafficking, in *Current Protocols in Cell Biology*, pp 15.2.1−15.2.26, John Wiley and Sons, Inc., New York.
25. Hayes, G. R., Williams, A. M., Lucas, J. J., and Enns, C. A. (1997) Structure of human transferrin receptor oligosaccharides: conservation of site-specific processing. *Biochemistry 36*, 5276–5284.
26. Mollenhauer, H. H., Morre, D. J., and Rowe, L. D. (1990) Alteration of intracellular traffic by monensin; mechanism, specificity and relationship to toxicity. *Biochim. Biophys. Acta 1031*, 225–246.
27. Uchida, N., Smilowitz, H., and Tanzer, M. L. (1979) Monovalent ionophores inhibit secretion of procollagen and fibronectin from cultured human fibroblasts. *Proc. Natl. Acad. Sci. U.S.A. 76*, 1868–1872.
28. Lippincott-Schwartz, J., Yuan, L. C., Bonifacino, J. S., and Klausner, R. D. (1989) Rapid redistribution of Golgi proteins into the ER in cells treated with brefeldin A: evidence for membrane cycling from Golgi to ER. *Cell 56*, 801–813.
29. Liu, X. M., Peyton, K. J., Ensenat, D., Wang, H., Schafer, A. I., Alam, J., and Durante, W. (2005) Endoplasmic reticulum stress stimulates heme oxygenase-1 gene expression in vascular smooth muscle. Role in cell survival. *J. Biol. Chem. 280*, 872–877.
30. Rab, A., Bartoszewski, R., Jurkuvenaite, A., Wakefield, J., Collawn, J. F., and Bebok, Z. (2007) Endoplasmic reticulum stress and the unfolded protein response regulate genomic cystic fibrosis transmembrane conductance regulator expression. *Am. J. Physiol. Cell Physiol. 292*, C756−C766.
31. Crawford, P. A., Gaddie, K. J., Smith, T. M., and Kirley, T. L. (2007) Characterization of an alternative splice variant of human nucleoside triphosphate diphosphohydrolase 3 (NTPDase3): A

possible modulator of nucleotidase activity and purinergic signaling. *Arch. Biochem. Biophys. 457*, 7–15.
32. Teasdale, R. D., and Jackson, M. R. (1996) Signal-mediated sorting of membrane proteins between the endoplasmic reticulum and the golgi apparatus. *Annu. Rev. Cell. Dev. Biol. 12*, 27–54.
33. Jackson, M. R., Nilsson, T., and Peterson, P. A. (1993) Retrieval of transmembrane proteins to the endoplasmic reticulum. *J. Cell. Biol. 121*, 317–333.
34. Hauri, H. P., Kappeler, F., Andersson, H., and Appenzeller, C. (2000) ERGIC-53 and traffic in the secretory pathway. *J. Cell Sci. 113*, 587–596.
35. Andersson, H., Kappeler, F., and Hauri, H. P. (1999) Protein targeting to endoplasmic reticulum by dilysine signals involves direct retention in addition to retrieval. *J. Biol. Chem. 274*, 15080–15084.
36. Knowles, A. F., and Chiang, W. C. (2003) Enzymatic and transcriptional regulation of human ecto-ATPase/E-NTPDase 2. *Arch. Biochem. Biophys. 418*, 217–227.
37. Clairmont, C. A., De Maio, A., and Hirschberg, C. B. (1992) Translocation of ATP into the lumen of rough endoplasmic reticulum-derived vesicles and its binding to luminal proteins including BiP (GRP 78) and GRP 94. *J. Biol. Chem. 267*, 3983–3990.
38. Shin, S. J., Lee, W. K., Lim, H. W., and Park, J. (2000) Characterization of the ATP transporter in the reconstituted rough endoplasmic reticulum proteoliposomes. *Biochim. Biophys. Acta 1468*, 55–62.
39. Brockmeier, A., and Williams, D. B. (2006) Potent lectin-independent chaperone function of calnexin under conditions prevalent within the lumen of the endoplasmic reticulum. *Biochemistry 45*, 12906–12916.
40. Zebisch, M., and Strater, N. (2007) Characterization of rat NTPDase1, -2, and -3 ectodomains refolded from bacterial inclusion bodies. *Biochemistry 46*, 11945–11956.
41. Ward, C. L., and Kopito, R. R. (1994) Intracellular turnover of cystic fibrosis transmembrane conductance regulator. Inefficient processing and rapid degradation of wild-type and mutant proteins. *J. Biol. Chem. 269*, 25710–25718.
42. Nehls, S., Snapp, E. L., Cole, N. B., Zaal, K. J., Kenworthy, A. K., Roberts, T. H., Ellenberg, J., Presley, J. F., Siggia, E., and Lippincott-Schwartz, J. (2000) Dynamics and retention of misfolded proteins in native ER membranes. *Nat. Cell Biol. 2*, 288–295.
43. de Silva, A., Braakman, I., and Helenius, A. (1993) Posttranslational folding of vesicular stomatitis virus G protein in the ER: involvement of noncovalent and covalent complexes. *J. Cell. Biol. 120*, 647–655.
44. Mulvey, M., and Brown, D. T. (1995) Involvement of the molecular chaperone BiP in maturation of Sindbis virus envelope glycoproteins. *J. Virol. 69*, 1621–1627.
45. Oyadomari, S., and Mori, M. (2004) Roles of CHOP/GADD153 in endoplasmic reticulum stress. *Cell Death Differ. 11*, 381–389.
46. Fu, Y., and Lee, A. S. (2006) Glucose regulated proteins in cancer progression, drug resistance and immunotherapy. *Cancer Biol. Ther. 5*, 741–744.
47. Lee, A. S. (2007) GRP78 induction in cancer: therapeutic and prognostic implications. *Cancer Res. 67*, 3496–3499.
48. Jamora, C., Dennert, G., and Lee, A. S. (1996) Inhibition of tumor progression by suppression of stress protein GRP78/BiP induction in fibrosarcoma B/C10ME. *Proc. Natl. Acad. Sci. U.S.A. 93*, 7690–7694.
49. Park, H. R., Tomida, A., Sato, S., Tsukumo, Y., Yun, J., Yamori, T., Hayakawa, Y., Tsuruo, T., and Shin-ya, K. (2004) Effect on tumor cells of blocking survival response to glucose deprivation. *J. Natl. Cancer Inst. 96*, 1300–1310.
50. Dong, D., Ni, M., Li, J., Xiong, S., Ye, W., Virrey, J. J., Mao, C., Ye, R., Wang, M., Pen, L., Dubeau, L., Groshen, S., Hofman, F. M., and Lee, A. S. (2008) Critical role of the stress chaperone GRP78/BiP in tumor proliferation, survival, and tumor angiogenesis in transgene-induced mammary tumor development. *Cancer Res. 68*, 498–505.

BI800402Q